Xin *et al.*
EURASIP Journal on Advances in Signal Processing (2023) 2023:117
https://doi.org/10.1186/s13634-023-01079-y

EURASIP Journal on Advances in Signal Processing

RESEARCH Open Access

Comprehensive analysis of aero-engine vibration signals based on wavelet transform method

Mai Xin[1*], Zhifeng Ye[1], Yu Zhao[2], Xing Liu[1], Longlong Liu[1], Hailang Ge[1] and Tong Zhang[1]

*Correspondence:
xinmai_xm@nuaa.edu.cn

[1] College of Energy and Power Engineering, Jiangsu Province Key Laboratory of Aerospace Power System, Nanjing University of Aeronautics and Astronautics, 29 Yudao St, Nanjing 210016, People's Republic of China
[2] Xi'an Research Institute of Precision Machinery, Xi'an 7100752, People's Republic of China

Abstract

A single type of signal processing means that it is difficult to analyze vibration signals comprehensively and effectively. By comprehensively using wavelet analysis techniques, a comprehensive and in-depth study of aero-engine vibration conditions is realized as a way to carry out health management. By introducing various types of wavelet analysis techniques and using Labview2022 programming, corresponding signal processing tools are developed for the analysis of the collected vibration signals. The comprehensive analysis of aero-engine vibration signals based on the wavelet transform method is realized, and the corresponding products are successfully applied in engineering practice.

Keywords: Aero-engine, Vibration signal, Wavelet transform method, Fault analysis

1 Introduction

Aero-engine is an extremely precise industrial product, which is difficult and costly to develop [1]. Aero-engine is the core component of the aircraft, whose good condition is related to the safety and reliability of the aircraft. Therefore, the maintenance requirements of the aircraft engine are high [2].

For industrial products, process-wise, frequent disassembly, and installation during maintenance is detrimental to the reliability of the equipment and can even lead to fatigue of the mechanical components, thus endangering the safety of the equipment [3, 4]. Therefore, nondestructive testing by radiation detection, electromagnetic testing, and vibration testing has received a great deal of attention in the field of engineering technology. The study of aero-engine working conditions by vibration signal measurement is considered the most intuitive and effective inspection method in the industry [5, 6].

However, for signal analysis, it is often difficult to use a single analysis method to achieve the purpose of comprehensive investigation, and it will show its disadvantage when analyzing the signal of a specific condition. Therefore, here we introduce a variety of analysis methods based on wavelet transform to achieve the goal of comprehensive analysis of the signal. In this study, LabVIEW2022 is used to develop

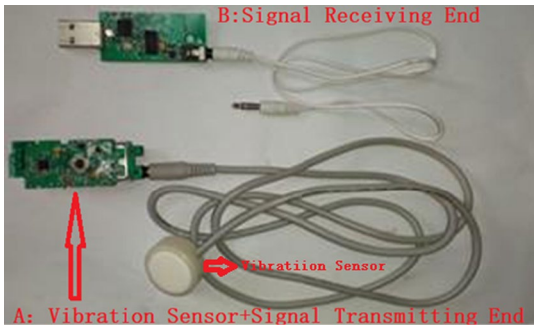

Fig. 1 The physical picture of vibration signal wireless acquisition module

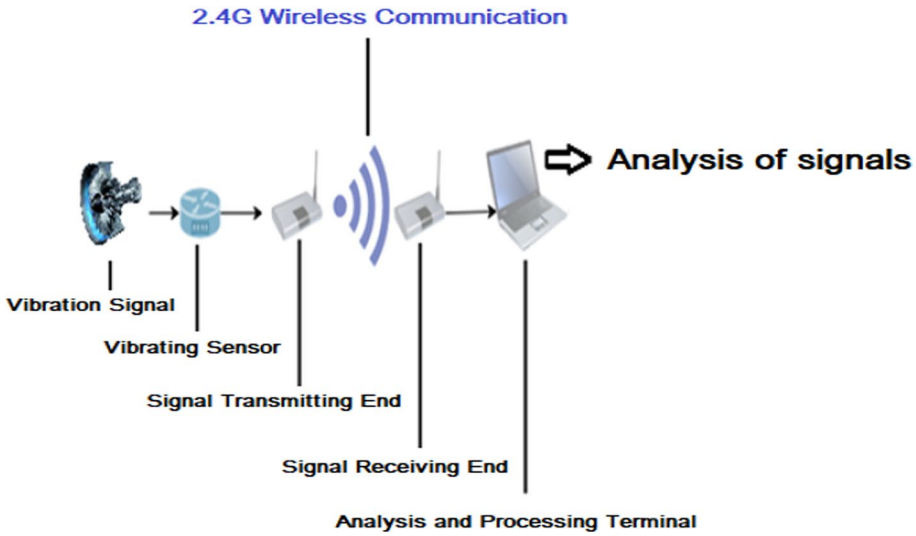

Fig. 2 The schematic of system functional design

signal processing tools, and a certain type of aero-engine is used as an experimental measurement object for diagnostic analysis.

2 Design and implementation of system functions

2.1 Function designs

By applying the previously designed vibration signal wireless acquisition module based on 2.4G technology development (shown in Fig. 1), the aero-engine vibration signal is acquired and stored in the computer for analysis.

The wavelet transform window changes with the change of frequency and incorporates the idea of Fourier local transform, which can be used to analyze the signal by highlighting the features of the corresponding aspects flexibly through the transform [7, 8]. The specific analysis functions are developed based on wavelet transform, and there are three types: multi-resolution analysis based on discrete wavelet transform; multi-scale analysis based on wavelet transform; and two-dimensional wavelet transform analysis. The functional design of the system is shown in Fig. 2.

2.2 Principle of analysis tools

2.2.1 Principle of multi-resolution analysis based on discrete-time wavelet transform

Signal flow exists in a discrete signal pattern in a computer. The multi-resolution discrete wavelet transform analysis can be represented in the following concrete form [9, 10]. Let $\{V_j\}$ be a series of closed subspaces in $L^2(R)$ with $j \in Z$. To claim that $\{V_j\}$, $j \in z$ is a multi-resolution analysis, the following six conditions must be satisfied simultaneously [11].

① There exists $(j,k) \in Z^2$ with $x(t) \in V_j$, then $x(t-2^j k) \in V_j$
② There exists $j \in Z, v_j \supset v_{j+1}$, i.e. $\cdots V_0 \supset V_1 \supset \cdots v_j \supset v_{j+1} \cdots$
③ There exists $j \in Z$, if $x(t) \in V_j$, then $x\left(\frac{t}{2}\right) \in v_{j+1}$
④
$$V_j = \bigcap_{j=-\infty}^{\infty} V_j = \{0\} \tag{1}$$

⑤
$$V_j = \text{Closure}\left(\bigcup_{j=-\infty}^{\infty} V_j\right) = L^2(R) \tag{2}$$

⑥ There exists $\theta(t)$, such that $\{\theta(t-k)\}$ the Riesz basis in V_0 and $k \in Z$

Let V_0 be a Hilbert space and $\{\theta_k = \theta(t-k)\}, k \in Z$ be a set of vectors in V_0 whose number is the same as the dimension of V_0. Any element x in V_0 can be tabulated as a linear combination of θ_k [12].

$$x(t) = \sum_{k=\infty}^{\infty} c_k \theta(t-k) \tag{3}$$

If

$$\{\theta_k = \theta(t-k)\}, k \in Z \tag{4}$$

is linearly independent and there exists a constant $0 < A \le B < \infty$ such that

$$A\|x\|^2 \le \sum_{k=\infty}^{\infty} |c_k|^2 \le B\|x\|^2 \tag{5}$$

Then $\{\theta_k = \theta(t-k)\}, k \in Z$ is the Riesz basis in V_0 [11].

Let $\{V_j\}, j \in Z$ be a multi-resolution analysis and $\phi(t)$ be a scale function. If its Fourier transform can be given by the following equation

$$\Phi(\Omega) = \frac{\hat{\theta}(\Omega)}{\left[\sum_{k=-\infty}^{\infty} |\hat{\theta}(\Omega + 2k\pi)|^2\right]^{1/2}} \tag{6}$$

and make

$$\phi_{j,k}(t) = 2^{-j/2}\phi\left(2^{-j}t - k\right) \tag{7}$$

Then, $\phi_{j,k}(t)$ is an orthogonal normalized basis in V_j for all $j \in Z$.

2.2.2 Principles of wavelet transform multi-scale analysis

The multi-scale analysis consists of a column of subspaces $\{V_j\}, j \in Z$ of $L^2(R)$, where $L^2(R)$ denotes the Hilbert space of all square productable functions, and R and Z denote the set of real numbers and the set of integers, respectively [13–15]. The multi-resolution analysis allows to establish the dual scale equation of the scale function $\phi(t)$, i.e., the scale function at one scale can be derived from its own linear combination at the next scale [16–18]. The scale function and the wavelet mother function are related to each other, and the wavelet mother function $\psi(t)$ can be obtained from the scale function $\phi(t)$.

$$\varphi(t) = \sqrt{2}\sum_{n\in Z} h_n \varphi(2t-n) \tag{8}$$

h_n is the scale function

$$\psi(t) = \sqrt{2}\sum_{n\in Z} g_n \varphi(2t-n) \tag{9}$$

where $\sqrt{2}$ is the normalization factor and g_n is the coefficient derived from the scale factor h_n.

Let $\psi_{j,k}(t)$ be the expansion and translation of the wavelet mother function $\psi(t)$, and $\psi_{j,k}(t)$ form the orthogonal basis of f. $\phi_{ok}(t)$ is a telescoping translation of the ruler function $\phi(t)$, then at any $f(t) \in L^2(R)$, it can be decomposed as:

$$f(t) = \sum_{k\in Z} c_k \phi_{ok}(t) + \sum_{j<J,k\in Z} d_{j,k}\psi_{J,k}(t) \tag{10}$$

Among them,

$$c_k = \int_R f(t)\phi_{ok}(t)\mathrm{d}t \tag{11}$$

$$d_{j,k} = \int_R f(t)\psi_{j,k}(t)\mathrm{d}t \tag{12}$$

J controls the resolution of the wavelet analysis.

2.2.3 Principle of two-dimensional wavelet transform analysis

Since image and computer vision signals are generally two- or multidimensional information, it is important to extend the signal analysis to two or more dimensions [19–21].

① Definition

Let $f(x,y) \in L^2(R^2)$, then its two-dimensional wavelet transform is:

$$W_f(a,b_1,b_2)=\int_{-\infty}^{+\infty}\int_{-\infty}^{+\infty}f(x,y)\frac{1}{a}\overline{\psi}\left(\frac{x-b_1}{a},\frac{y-b_1}{a}\right)\mathrm{d}x\mathrm{d}y \tag{13}$$

where b_1, b_2 are the translation values of the basic wavelet function in two dimensions, and the two-dimensional wavelet function $\psi(x,y)$ should satisfy the tolerance condition:

$$\int_{-\infty}^{+\infty}\int_{-\infty}^{+\infty}\psi(x,y)\mathrm{d}x\mathrm{d}y=0 \tag{14}$$

It can be shown that the corresponding reconfiguration equation is

$$f(x,y)=\frac{1}{C_\psi}\int_{-\infty}^{+\infty}\int_{-\infty}^{+\infty}\int_{-\infty}^{+\infty}a^{-3}W_f(a,b_1,b_2)\psi\left(\frac{x-b_1}{a},\frac{y-b_2}{a}\right)\mathrm{d}a\mathrm{d}b_1b_2 \tag{15}$$

Discrete wavelet transform is obtained by discretizing the parameters a, b in Eq. (15): $a=2^j$, $b_1=al$, $b_2=am$:

$$W_f(j,l,m)=2^{-j}\int_{-\infty}^{+\infty}\int_{-\infty}^{+\infty}f(x,y)\overline{\psi}\left(2^{-j}x-l,2^{-j}y-m\right)\mathrm{d}x\mathrm{d}y \tag{16}$$

In practice, commonly used wavelet functions are binary functions with separable variables.

$$\psi(x,y)=\psi_1(x)\psi_2(y) \tag{17}$$

Two-dimensional multi-scale analysis is derived from one-dimensional multi-scale analysis, which in turn leads to two-dimensional wavelet space and wavelet function.

Let $\left(\left\{V_j^1(t)\right\}_{j\in Z},\varphi^1(t)\right)$, $\left(\left\{V_j^2(t)\right\}_{j\in Z},\varphi^2(t)\right)$ be two multi-scale analyses of $L^2(R^2)$, and $\psi^1(t)$, $\psi^2(t)$ be the corresponding orthogonal wavelet functions. The tensor product space formed by V_j^1 and V_j^2 is defined as

$$\tilde{V}_j=V_j^1\otimes V_j^2=\left\{f(x)g(y)\middle|f(x)\in V_j^1,g(x)\in V_j^2\right\} \tag{18}$$

Let W_j^1 be the orthogonal complementary space of V_j^1 in V_{j-1}^1 and W_j^2 be the orthogonal complementary space of V_j^2 in V_{j-1}^2, then we have the following expressions [22].

$$\begin{aligned}\tilde{V}_{j-1}&=V_{j-1}^1\otimes V_{j-1}^2=\left(V_j^1\oplus W_j^1\right)\otimes\left(V_j^2\oplus W_j^2\right)\\&=\left(V_j^1\otimes V_j^2\right)\oplus\left(W_j^1\otimes V_j^2\right)\oplus\left(V_j^1\otimes W_j^2\right)\oplus\left(W_j^1\otimes W_j^2\right)=\tilde{V}_j\oplus\tilde{W}_j^1\oplus\tilde{W}_j^2\oplus\tilde{W}_j^3\end{aligned} \tag{19}$$

② Reconstruction formula for two-dimensional wavelets

From the definition of 1-D multi-scale analysis there are

$$\{0\}\subseteq\cdots\subseteq\tilde{V}_1\subseteq\tilde{V}_0\subseteq\tilde{V}_{-1}\subseteq\cdots L^2\left(R^2\right),\ \bigcap_{j\in Z}\tilde{V}_j=\{0\},\bigcup_{j\in Z}\tilde{V}_j=L^2\left(R^2\right) \tag{20}$$

Thus, the sequence of subspaces $\left\{\tilde{V}_j\right\}_{j\in Z}$ satisfies the definition of multi-scale analysis, and thus we obtain a multi-scale analysis of the two-dimensional space $(\left\{\tilde{V}_j\right\}_{j\in Z},\varphi(x,y))$.

$$L^2\left(R^2\right) = \cdots \oplus \tilde{W}_{-j} \oplus \tilde{W}_0 \oplus \tilde{W}_{1\oplus} \cdots \tag{21}$$

of which

$$\tilde{W}_j = \tilde{W}_j^1 \oplus \tilde{W}_j^2 \oplus \tilde{W}_j^3 \tag{22}$$

Therefore, for any $f(x,y) \in L^2(R^2)$ there is a unique decomposition.

$$f(x,y) = \cdots + g_{-1}(x,y) + g_0(x,y) + g_1(x,y) + \cdots \tag{23}$$

where $g_j(x,y) \in \tilde{W}_j$, so the following expressions are available.

$$f(x,y) = \sum_{j=-\infty}^{+\infty} \sum_{k,m} \left[a_{k,m}^j \psi_{j,k}^1(x)\varphi_{j,m}^2(y) + \beta_{k,m}^j \varphi_{j,k}^1(x)\psi_{j,m}^2(y) + \gamma_{k,m}^j \psi_{j,k}^1(x)\psi_{j,m}^2(y)\right] \tag{24}$$

From orthogonality it is known that

$$a_{k,m}^j = \iint_{R^2} f(x,y)\overline{\psi_{j,k}^1}(x)\overline{\varphi_{j,m}^2}(y)\mathrm{d}x\mathrm{d}y \tag{25}$$

$$\beta_{k,m}^j = \iint_{R^2} f(x,y)\overline{\varphi_{j,k}^1}(x)\overline{\psi_{j,m}^2}(y)\mathrm{d}x\mathrm{d}y \tag{26}$$

$$\gamma_{k,m}^j = \iint_{R^2} f(x,y)\overline{\psi_{j,k}^1}(x)\overline{\psi_{j,m}^2}(y)\mathrm{d}x\mathrm{d}y \tag{27}$$

From the definition of two-dimensional wavelet transform, we know that $a_{k,m}^j$, $\beta_{k,m}^j$, $\gamma_{k,m}^j$ are two-dimensional discrete wavelet transforms of $f(x,y)$; $\psi^1(x,y)$, $\psi^2(x,y)$, $\psi^3(x,y)$ are three different wavelet functions, all of them are functions of variable separation type consisting of a one-dimensional wavelet function and a scale function [23–25].

$$\varphi(x,y) = \varphi^1(x)\varphi^2(y) \tag{28}$$

is the scale function corresponding to the three different wavelet functions.

2.3 Programming design

The project team used LabVIEW2022 to develop and implement functions based on discrete wavelet transform multi-resolution analysis, wavelet transform-based multi-scale analysis, and two-dimensional wavelet transform analysis.

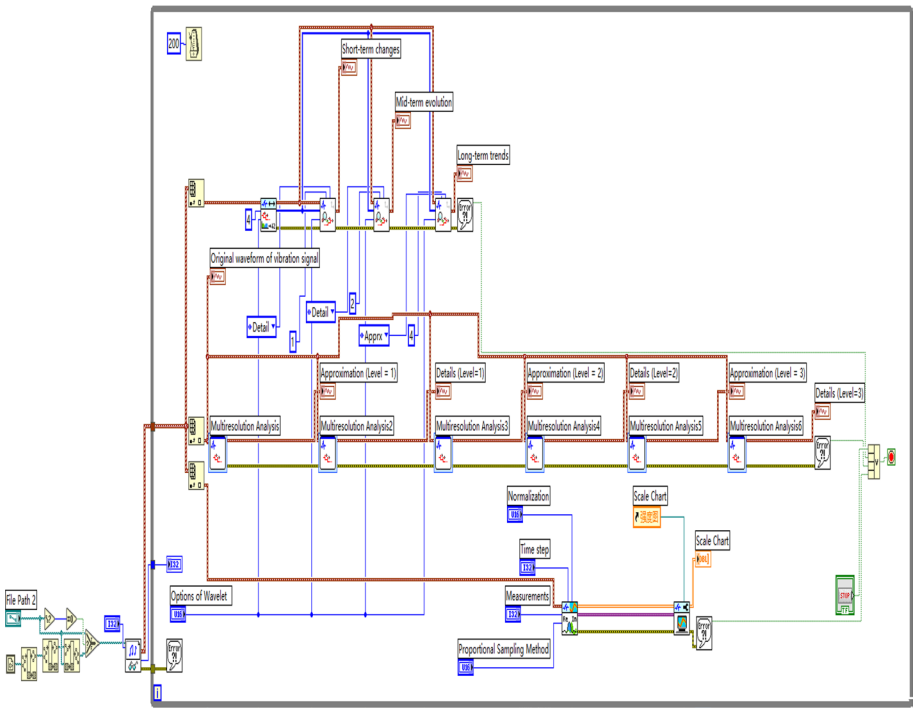

Fig. 3 The program panel diagram of system

The system enables a comprehensive study of the signals, allowing engineers to have a deeper grasp of the vibration of the aero-engine under test. In this way, it can determine the working status of the aero-engine, realize the fault diagnosis, and play the role of health management. The program panel is shown in Fig. 3.

3 Experiments and discussion

3.1 Experiment I

A model of a small aero-engine (teaching prototype) was used as the experiment object. By starting the engine on the ground bench, the project team collected its vibration signal in normal operation (economic cruise state) as the normal reference signal. By setting the engine stuck fault, its vibration signal in that operation state was collected and compared with the former for illustration.

As shown in Fig. 4, the upper panel is the result screen of running a normal reference signal; the lower panel is the result screen of running a stuck fault vibration signal. The system interface presents a combination of four display frames: the original waveform map of the signal, the discrete wavelet transform-based multi-resolution analysis map, the wavelet transform-based multi-scale analysis map, and the two-dimensional wavelet transform analysis map. In general, each analysis method can effectively deduce the characteristics of the signal. When this type of aero-engine is in cruise, the signal shows smoothness, indicating that the unit is running steadily; when it is in a stuck state, the plot boxes of each method demonstrate the corresponding state characteristics.

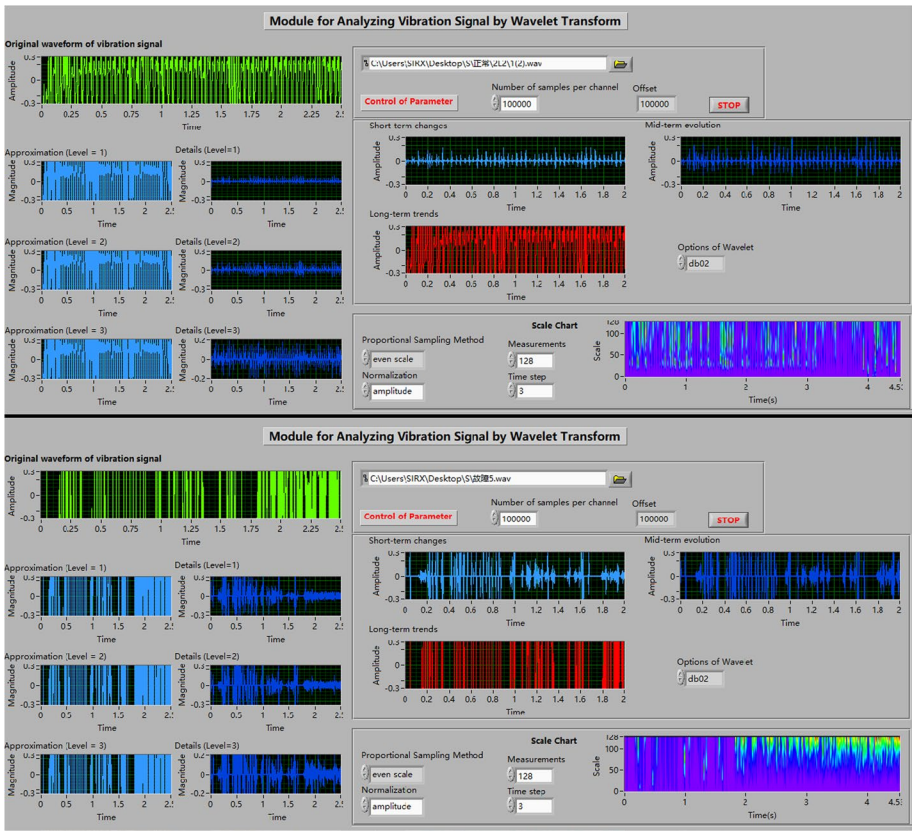

Fig. 4 The overall result interface of experiment I

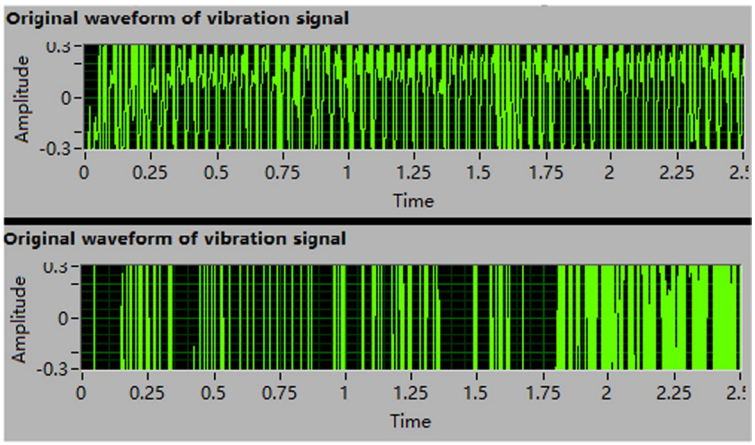

Fig. 5 Experiment I: Comparison of the original waveform diagram of the signals

As shown in Fig. 5, the upper figure is the original waveform of the normal reference signal, and the lower figure is the original waveform of the vibration signal when the engine is in a stuck fault condition. The two can be clearly distinguished from each other by the smoothness of the signal.

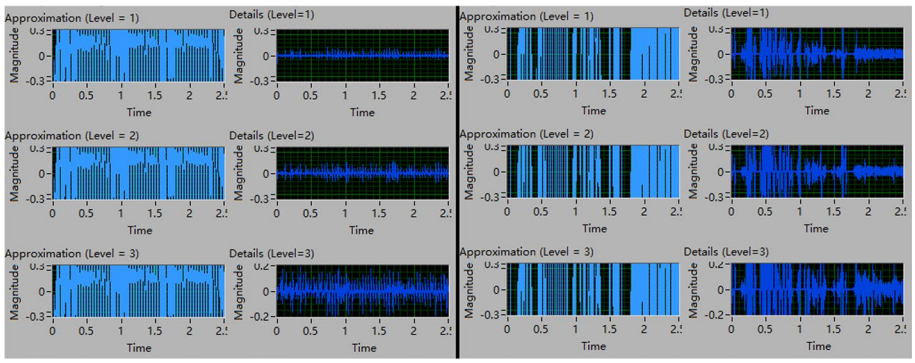

Fig. 6 Experiment I: Multi-resolution analysis of signals based on discrete wavelet transform

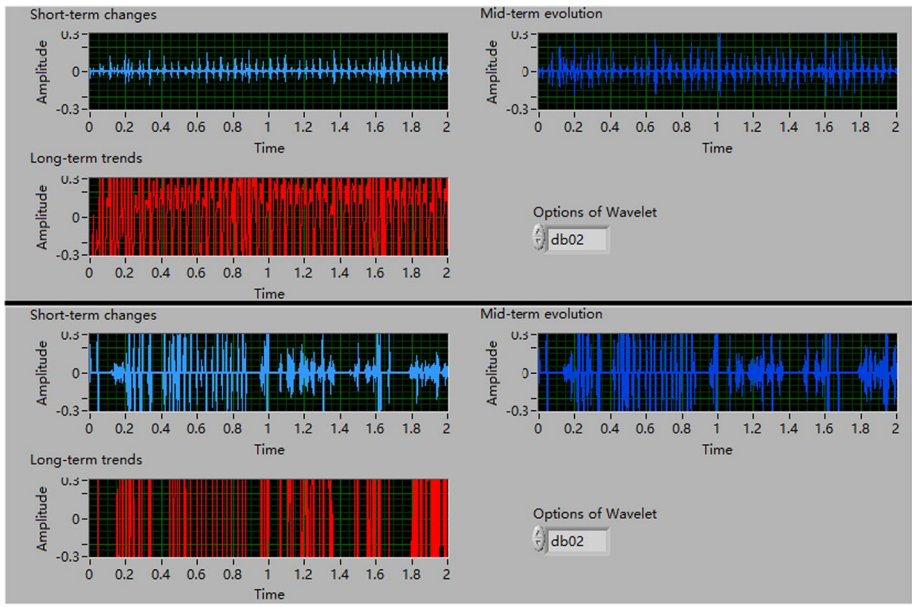

Fig. 7 Experiment I: Wavelet transform multi-scale analysis of signals

As shown in Fig. 6, the left and right figures show the results based on the discrete wavelet transform multi-resolution analysis of the above signals: the left figure presents the results for the normal reference signal, and the right figure presents the results when it is in a stuck fault condition. There is a clear distinction between the two features.

As shown in Fig. 7, two signals are presented based on the multi-scale analysis of the wavelet transform: the upper panel shows the results of the analysis of the normal reference signal; the lower panel shows the results of the analysis of the signal when the engine is in a stuck fault condition. The interface has 3 display windows, and the differences between the two are very obvious when examined in terms of the periodicity and smoothness of the signals.

As shown in Fig. 8, what is presented is a plot of the signal after analysis by 2D wavelet transform: the upper plot is the result of analyzing the normal baseline signal; the lower plot is the result of analyzing the signal when the engine is in a stuck

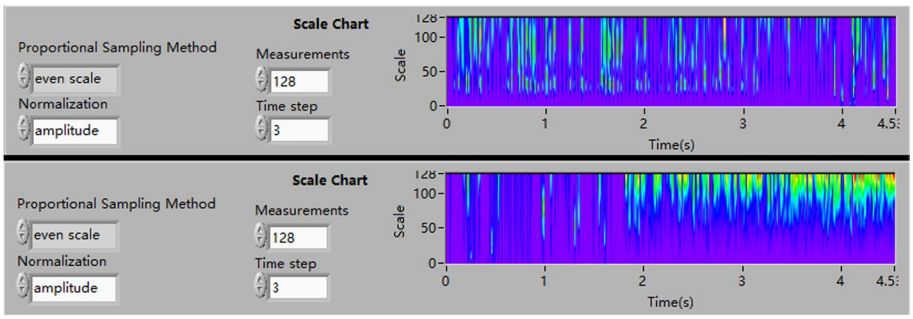

Fig. 8 Experiment I: Analysis by two-dimensional wavelet transform for signals

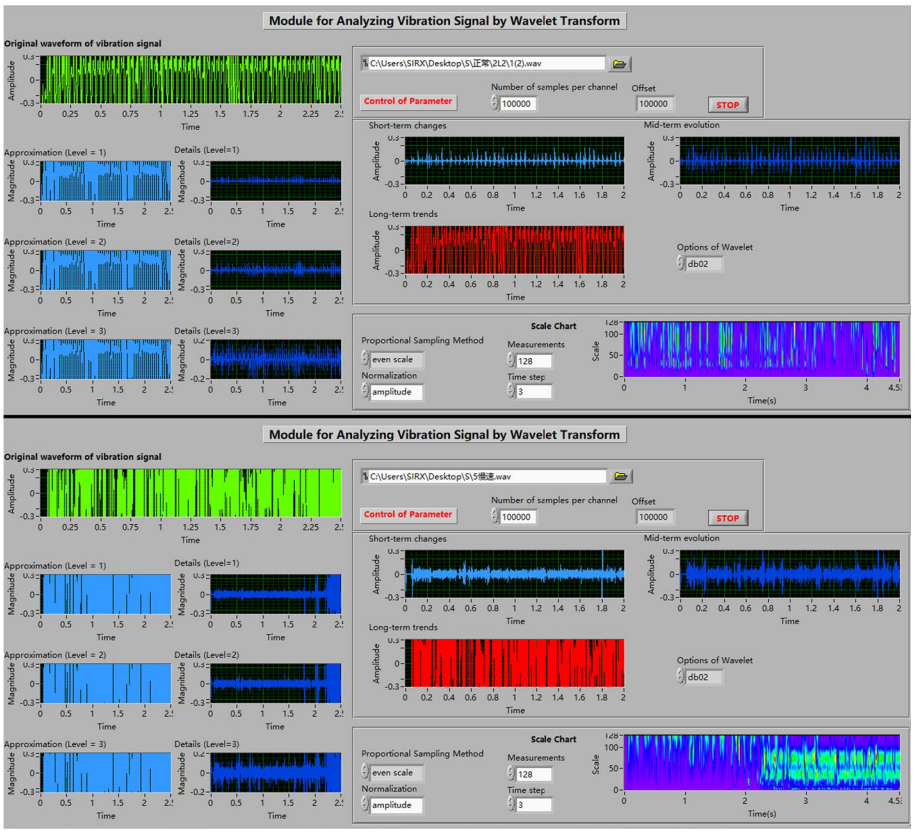

Fig. 9 Overall results interface for Experiment II

fault condition. Two-dimensional mapping has the property of showing the energy condition of the signal, so it is practical to examine the signal condition from the smoothness of the signal and the regularity of the energy distribution. The normal reference signal has good smoothness, and the energy distribution shows obvious regularity; while in the stuck fault state, the signal smoothness is poor and the energy distribution varies widely. The differences between the above two signals are obvious.

3.2 Experiment II

According to the same conditions as the previous experiment, a model of a small aero-engine (teaching prototype) was used as the experimental object. Fixed on the ground bench to start, the project team collected its vibration signal in normal operation (economic cruise state) as the normal reference signal. By setting up an engine sticky fault, the project team collected its vibration signal in that operating condition and compared it with the former for illustrative purposes.

As shown in Fig. 9, the upper panel is the result screen of running a normal reference signal; the lower panel is the result screen of running a sticky fault vibration signal. When this type of aero-engine is in a sticky state, the signal shows smoothness and a certain regularity in the energy distribution from the operation results of individual analysis methods. However, operation in a sticky state is also a fault.

As shown in Fig. 10, the upper figure is the original waveform of the normal reference signal, and the lower figure is the original waveform of the vibration signal when the engine is in sticking condition. From the characteristics of the waveform, the waveform

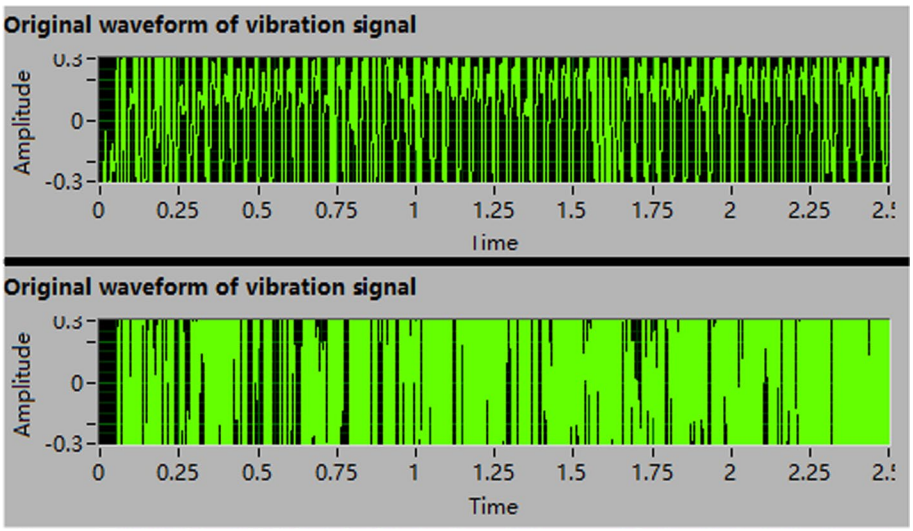

Fig. 10 Experiment II: Comparison of the original waveform diagram of the signals

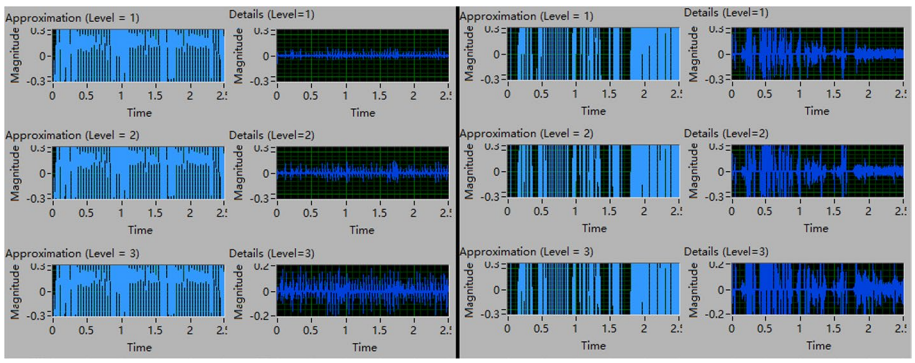

Fig. 11 Experiment II: Multi-resolution analysis of signals based on discrete wavelet transform

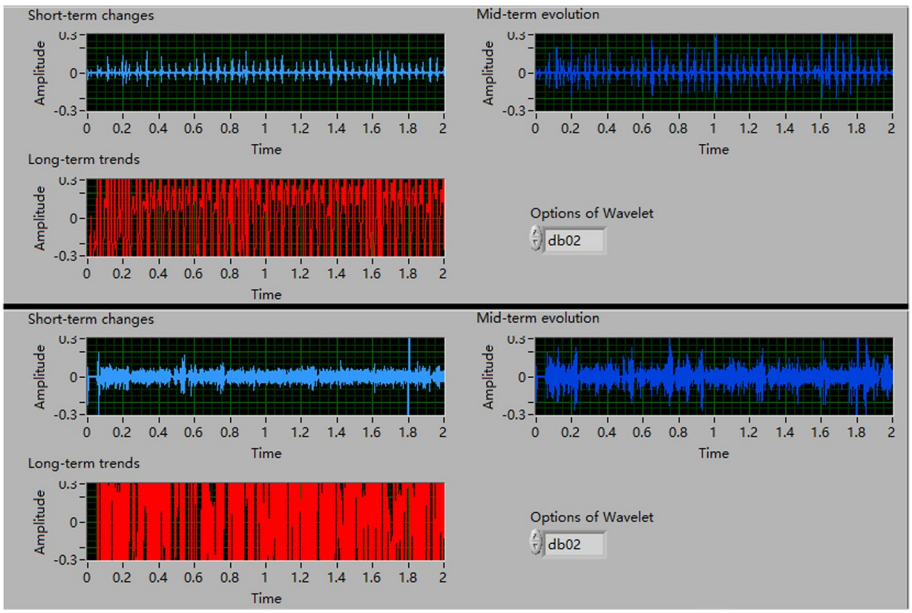

Fig. 12 Experiment II: Wavelet transform multi-scale analysis of signals

graph of the vibration signal in the sticky state already has a certain smoothness. The differentiation of the signal characteristics is not as obvious as the previous stuck signal waveform. Therefore, it will affect the accuracy of fault determination using this tool.

As shown in Fig. 11, the left and right plots show the results based on the discrete wavelet transform multi-resolution analysis of the above signal. The left figure presents the results for the normal reference signal, while the right figure presents the results when it is in the sticky state. The features between the two are clearly distinguished.

As shown in Fig. 12, two signals are presented based on the multi-scale analysis of wavelet transform. The top panel is the result of analyzing the normal reference signal; the bottom panel is the result of analyzing the signal when the engine is in a sticky state. The interface has 3 display windows, and the differences between both are very obvious when examined in terms of the periodicity and smoothness of the signals, but the signal in the sticky state shows good periodicity and smoothness. The distinguishability appears weaker than the previous card resistance signal. Therefore, it can affect the accuracy of the judgment using this tool.

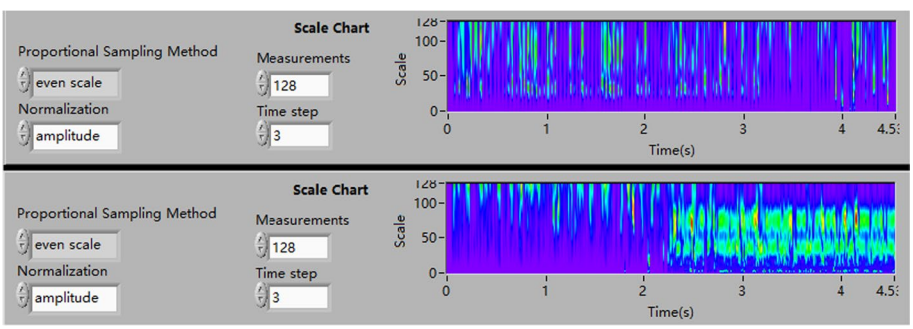

Fig. 13 Experiment II: Analysis by two-dimensional wavelet transform for signals

As shown in Fig. 13, the plot is presented after the signal is analyzed by two-dimensional wavelet transform. The upper figure is the result of analyzing the normal reference signal; the lower figure is the result of analyzing the signal when the engine is in a sticky state. Although the plots of signals in the sticky state after processing by this method are somewhat distinguishable from those formed by the constant reference signal, they are more similar to the signals generated in the stuck state (as shown in Fig. 8) and are not very easy to distinguish. Therefore, it is not reliable to use this method as a single criterion for fault type. By combining multiple analysis methods, we can analyze the signal comprehensively to achieve fault diagnosis and effective identification.

4 Conclusion

This study uses LabVIEW2022 to successfully implement a system for comprehensive analysis of aero-engine vibration signals based on the wavelet transform method, which can quickly carry out fault diagnosis based on aero-engine, and the design has achieved the expected goal.

The practical application proves that all sub-functions of the system can be operated effectively. For different processing requirements, the system can also flexibly set each parameter for detailed analysis. The tool has successfully served the front-line work and has been unanimously recognized and welcomed by engineers and technicians in related fields.

By using wireless communication technology and a wavelet analysis tool developed based on LABVIEW, the research team successfully realized wireless monitoring and troubleshooting of an aero-engine. In terms of design and application, the system, on the one hand, is able to monitor the operation of the aero-engine and, on the other hand, is able to carry out auxiliary diagnostics of the type of faults based on the visualization and analysis of the signals.

Acknowledgements
We would like to express our deep gratitude for the strong support provided by Nanjing Univ Aeronaut & Astronaut, Coll Energy & Power Engn, Jiangsu Prov Key Lab Aerosp Power Syst.

Funding
This research was supported by the 'Innovation Research Fund for Doctoral Students of Nanjing University of Aeronautics and Astronautics,''National Natural Science Foundation of China,' and 'Funding of Jiangsu Innovation Program for Graduate Education.'

Availability of data and materials
The original data have been stored in" https://figshare.com/articles/figure/PIC-3/21724298".

Declarations

Competing interests
The authors declare that they have no known competing financial interests or personal relationships that could have appeared to influence the work reported in this paper.

Received: 15 June 2023 Accepted: 30 October 2023
Published: 15 November 2023

References

1. N. Melchert, M.K.B. Weiss, T. Betker, W. Frackowiak, R. Gansel, L. Keunecke, E. Reithmeier, H.J. Maier, M. Kästner, D. Zaremba, Combination of optical metrology and non-destructive testing technology for the regeneration of aero engine components. Tech. Mess.: Sens. Gerate Syst. **88**(4), 237–250 (2021)
2. L.I. Zhen, S. Zhong, L. Lin, An aero-engine life-cycle maintenance policy optimization algorithm: the reinforcement learning approach. Chin. J. Aeronaut. **32**(9), 2133–2150 (2019)

3. F. Fang, H. Zheng, Y. Wang, L. Qiu, Mechanical Structural health monitoring: a review. J. Mech. Eng. **57**(16), 269–292 (2021)
4. M. Cao, P. Wang, H. Zuo, H. Zeng, J. Sun, W. Yang, F. Wei, X. Chen, Current status, challenges and opportunities of civil aero-engine diagnostics and health management II: comprehensive off-board diagnosis, life management and intelligent condition based mro. Acta Aeronautica et Astronautica Sinica **43**(9), 42–81 (2022)
5. J. Liu, H. Zhang, J. Zhai, Q. Han, Nonlinear dynamic analysis of the central bevel gear transmission system in aero engine subjected to internal and external excitation. Proc. Inst. Mech. Eng. C J. Mech. Eng. Sci. **236**(11), 5940–5953 (2022)
6. M. Gambitta, A. Kühhorn, B. Beirow, S. Schrape, Stator blades manufacturing geometrical variability in axial compressors and impact on the aeroelastic excitation forces. J. Turbomach. **144** (4), (2021)
7. A. Anwarsha, T. Babu, A review on the role of tunable Q-factor wavelet transform in fault diagnosis of rolling element bearings. J. Vib. Eng. Techn. **10**, 1793–1808 (2022)
8. A.P.C. de Sena, I.S. de Freitas, A.C.L. Filho, C.A.N. Sobrinho, Fuzzy diagnostics for gearbox failures based on induction motor current and wavelet entropy. J. Braz. Soc. Mech. Sci. Eng. **43**(5), 265 (2021)
9. T. Bandos, L. Bruzzone, G. Camps-Valls, Classification of hyperspectral images with regularized linear discriminant analysis. IEEE Trans. Geosci. Rem. Sens. **47**, 862–873 (2009)
10. R.C. Guido, Wavelets behind the scenes: practical aspects, insights, and perspectives. Phys. Rep. **985**, 1–23 (2022)
11. C.P. Pandey, P. Phukan, Continuous and discrete wavelet transforms associated with hermite transform. Int. J. Anal. Appl. **18**(4), 531–549 (2020)
12. J. Suárez de la Fuente, A weak Hilbert space that is a twisted Hilbert space. J Inst. Math. Jussieu **19**(3), 855–867 (2018)
13. K.P. Isaev, R.S. Yulmukhametov, Riesz Bases of normalized reproducing kernels in fock type spaces. Anal. Math. Phys. **12**(1), 11 (2021)
14. E. Guariglia, Primality, fractality, and image analysis. Entropy **21**, 304 (2019)
15. D. Sundararajan, *Discrete Wavelet Transform: A Signal Processing Approach* (Discretewavelet Transform: A Signal Processing Approach, 2015)
16. S. Reich, M.-T. Truong, T.N.H. Mai, The split feasibility problem with multiple output sets in Hilbert spaces. Optim. Lett. **14**, 2335–2353 (2020)
17. A.S. Minhas, S. Singh, A new bearing fault diagnosis approach combining sensitive statistical features with improved multiscale permutation entropy method. Knowl.-Based Syst. **218**, 106883 (2021)
18. X. Zheng, Y.Y. Tang, J. Zhou, A framework of adaptive multiscale wavelet decomposition for signals on undirected graphs. IEEE Trans. Sign. Process. **67**(7), 1696–1711 (2019)
19. E. Guariglia, R. Guido, Chebyshev wavelet analysis. J. Funct. Spaces **2022**, 1–17 (2022)
20. V.N. Ivanović, N.R. Brnović, Superior execution time design of a space/spatial-frequency optimal filter for highly nonstationary 2d Fm signal estimation. IEEE Trans. Circuits Syst. I Regul. Pap. **65**(10), 3376–3389 (2018)
21. X. Liu, H. Zhang, Y.-M. Cheung, X. You, Y.Y. Tang, efficient single image dehazing and denoising: an efficient multi-scale correlated wavelet approach. Comput. Vis. Image Underst. **162**, 23–33 (2017)
22. E. Guariglia, S. Silvestrov, Fractional-Wavelet analysis of positive definite distributions and wavelets on D′(C), in *Engineering Mathematics II.*, Springer, Cham, (2016)
23. E. Shipilova, M. Barret, M.R. Bloch, J.L. Boelle, J.-L. Collette, Simultaneous seismic sources separation based on Matrioshka orthogonal matching pursuit, application in oil and gas exploration. IEEE Trans. Geosci. Rem. Sens. **58**, 4529–4546 (2020)
24. C. Degen, Inductive coupling for wireless power transfer and near-field communication. EURASIP J. Wirel. Commun. Netw. **2021**(1), 121 (2021)
25. E. Guariglia, Harmonic Sierpinski gasket and applications. Entropy **20**(9), 714 (2018)

Publisher's Note